

This discussion paper is/has been under review for the journal Atmospheric Chemistry and Physics (ACP). Please refer to the corresponding final paper in ACP if available.

Observation of horizontal winds in the middle-atmosphere between 30° S and 55° N during the northern winter 2009–2010

P. Baron¹, D. P. Murtagh², J. Urban², H. Sagawa¹, S. Ochiai¹, H. Körnich³, F. Khosrawi⁴, K. Kikuchi¹, S. Mizobuchi⁵, K. Sagi², Y. Kasai^{1,6}, and M. Yasui¹

¹National Institute of Information and Communications Technology, 4-2-1 Nukui-kitamachi, Koganei, Tokyo 184-8795, Japan

²Department of Earth and Space Science, Chalmers University of Technology, 412 96 Göteborg, Sweden

³SMHI, Folkborgsvägen 1, 601 76 Norrköping, Sweden

⁴Department of Meteorology University of Stockholm 10691 Stockholm, Sweden

⁵Japan Aerospace Exploration Agency, Tsukuba, 305-8505 Japan

⁶Tokyo Institute of Technology, 4259 Nagatsuta-cho, Midori-ku, Yokohama, Kanagawa 226-8503, Japan

Title Page

Abstract

Introduction

Conclusions

References

Tables

Figures

◀

▶

◀

▶

Back

Close

Full Screen / Esc

Printer-friendly Version

Interactive Discussion



Received: 17 October 2012 – Accepted: 10 December 2012
– Published: 17 December 2012

Correspondence to: P. Baron (baron@nict.go.jp)

Published by Copernicus Publications on behalf of the European Geosciences Union.

ACPD

12, 32473–32513, 2012

SMILES winds

P. Baron et al.

Title Page

Abstract

Introduction

Conclusions

References

Tables

Figures



Back

Close

Full Screen / Esc

Printer-friendly Version

Interactive Discussion



Abstract

Although the links between stratospheric dynamics, climate and weather have been demonstrated, direct observations of stratospheric winds are lacking. We report observations of winds between 8 and 0.01 hPa ($\sim 35\text{--}80$ km) from October 2009 to April 2010 by the Superconducting Submillimeter-Wave Limb-Emission Sounder (SMILES) on the International Space Station. The altitude range covers the region between 35–60 km where previous space-borne wind instruments show a lack of sensitivity. Both zonal and meridional wind components were obtained, though not simultaneously, in the latitude range from 30° S to 55° N and with a single profile precision of 7–9 ms^{-1} between 8 and 0.6 hPa and better than 20 ms^{-1} at altitudes above. The vertical resolution is 5–7 km except in the upper part of the retrieval range (10 km at 0.01 hPa). In the region between 1–0.05 hPa, a mean difference $< 2 \text{ms}^{-1}$ is found between SMILES profiles retrieved from different spectroscopic lines and instrumental settings. Good agreement (mean difference of $\sim 2 \text{ms}^{-1}$) is also found with the European Centre for Medium-Range Weather Forecasts (ECMWF) analysis in most of the stratosphere except for the zonal winds over the equator (mean difference of 5–10 ms^{-1}). In the mesosphere, SMILES and ECMWF zonal winds exhibit large differences ($> 20 \text{ms}^{-1}$), especially in the tropics. We illustrate our results by showing daily and monthly zonal wind variations, namely the semi-annual oscillation in the tropics and reversals of the flow direction between 50° N–55° N during sudden stratospheric warmings in the stratosphere. The daily comparison with ECMWF winds reveals that in the beginning of February, a significantly stronger zonal westward flow is measured in the tropics at 2 hPa compared to the flow computed in the analysis (difference of $\sim 20 \text{ms}^{-1}$). The results show that the comparison between SMILES and ECMWF winds is not only relevant for the quality assessment of the new SMILES winds but it also provides insights on the quality of the ECMWF winds themselves. Although the instrument was not specifically designed for measuring winds, the results demonstrate that space-borne sub-mm wave radiometers

SMILES winds

P. Baron et al.

[Title Page](#)[Abstract](#)[Introduction](#)[Conclusions](#)[References](#)[Tables](#)[Figures](#)[◀](#)[▶](#)[◀](#)[▶](#)[Back](#)[Close](#)[Full Screen / Esc](#)[Printer-friendly Version](#)[Interactive Discussion](#)

have the potential to provide good quality data for improving the stratospheric winds in atmospheric models.

1 Introduction

Stratospheric winds play an important role in stratospheric chemistry by transporting long-lived species, or by creating transport barriers that for example isolate the polar vortex in winter (Shepherd, 2007, 2008). The stratospheric Quasi-biennial Oscillation (QBO) and downward feedback from the stratospheric vortex to tropospheric weather systems have also been reported to be relevant both in the context of weather prediction and climate (Baldwin and Dunkerton, 1999; Baldwin et al., 2003; Sigmond et al., 2008; Marshall and Scaife, 2009; Wang and Chen, 2010). In addition, stratospheric winds describe and affect vertically propagating atmospheric waves that control the transport circulation in the stratosphere and mesosphere (Holton and Alexander, 2000).

In meteorological analyses and reanalyses, unobserved variables are constrained by observed ones through the use of balance relationships. The application of a mass-wind balance (Derber and Bouttier, 1999) leads to a state where the large number of temperature soundings provide a strong constraint on the balanced wind component, i.e. approximately the geostrophic wind. However, this balance is not valid for non-geostrophic motion such as equatorial waves (Hamilton, 1998; Žagar et al., 2004) or for the middle atmospheric transport circulation (Polavarapu et al., 2005). A further complication in the middle atmosphere is that the small errors from the lower atmosphere propagate vertically and amplify strongly in the upper stratosphere and mesosphere (Nezlin et al., 2009; Alexander et al., 2010). Thus, in order to constrain middle atmospheric winds in meteorological analyses, global wind observations in the middle atmosphere are essential. Lahoz et al. (2005) have shown that wind observations on a global scale with a precision of 5 ms^{-1} between 25 and 40 km would provide

SMILES winds

P. Baron et al.

Title Page

Abstract

Introduction

Conclusions

References

Tables

Figures



Back

Close

Full Screen / Esc

Printer-friendly Version

Interactive Discussion



significant improvements of zonal-winds analyses especially in the tropical middle and upper stratosphere (50–1 hPa).

In spite of the importance of middle atmospheric observations, wind measurements assimilated in the models are mostly limited to the troposphere. In the mesosphere, winds are measured using optical techniques from satellites (Shepherd et al., 1993; Hays et al., 1993; Killeen et al., 1999; Swinbank and Ortland, 2003; Niciejewski et al., 2006) and by ground-based radar systems such as European Incoherent SCATter (EISCAT) (Alcaydé and Fontanari, 1986) and various meteor radars (Maekawa et al., 1993; Jacobi et al., 2009). Wu et al. (2008) have used the microwave oxygen line at 118 GHz measured by the Microwave Limb Sounder (MLS) to derive line-of-sight winds in the mesosphere (80–92 km). The authors suggested that winds can be derived down to 40 km by using emission lines from other molecules, but no results have been shown yet. Stratospheric winds have been measured from the ground using active and passive techniques (Hildebrand et al., 2012; Rüfenacht et al., 2012) and from space by the High Resolution Doppler Imager (HRDI) on UARS covering 10–35 km and 60° S–60° N, using the molecular oxygen A- and B-bands (Ortland et al., 1996).

Figure 1 summarises previous and planned wind measuring instruments from spaceborne platforms. A gap in the coverage of high quality winds ($< 5 \text{ ms}^{-1}$ error) between 30 and 60 km clearly exists. The ESA Atmospheric Dynamics Mission on the Aeolus satellite is planned for 2013–2014 (Stoffelen et al., 2005) for measuring winds in the troposphere and lower stratosphere using a IR/UV lidar. For middle-stratospheric winds, the Stratospheric Wind Interferometer For Transport studies (SWIFT) instrument was planned by the Space Canadian Agency for 2010 (McDade et al., 2001) but has an unclear future at the time of writing. The target of SWIFT is to measure the thermal emission from O_3 lines at $8 \mu\text{m}$ in order to provide winds on a near global scale between 15–50 km with the best accuracy of $3\text{--}5 \text{ ms}^{-1}$ between 20–40 km and a vertical resolution of 2 km.

Here we report the first spaceborne observations of winds in the altitude gap 30–60 km using the Superconducting Submillimeter-Wave Limb-Emission Sounder

SMILES winds

P. Baron et al.

Title Page

Abstract

Introduction

Conclusions

References

Tables

Figures

◀

▶

◀

▶

Back

Close

Full Screen / Esc

Printer-friendly Version

Interactive Discussion



SMILES winds

P. Baron et al.

[Title Page](#)[Abstract](#)[Introduction](#)[Conclusions](#)[References](#)[Tables](#)[Figures](#)[◀](#)[▶](#)[◀](#)[▶](#)[Back](#)[Close](#)[Full Screen / Esc](#)[Printer-friendly Version](#)[Interactive Discussion](#)

(SMILES) onboard the Japanese Experiment Module (JEM) of the International Space Station (ISS) (Kikuchi et al., 2010; Ochiai et al., 2012b). The instrument was launched in September 2009 for deriving trace gas profiles. Although SMILES was not designed for this purpose, we have exploited its high frequency resolution and high signal to noise ratio to derive the small Doppler shifts in the atmospheric spectra and thereby line-of-sight wind velocities. Because of the ISS rotation during an orbit, both zonal and meridional components ($\pm 10^\circ$) are retrieved between 30° S– 55° N. As shown in this analysis, the wind information is derived from 8–0.01 hPa (~ 35 – 80 km) with a precision better than 10 ms^{-1} at altitudes between 6 and 0.5 hPa and better than 20 ms^{-1} at altitudes above.

The main purpose of this paper is to present the wind data that has been derived from the six months of SMILES observations (October 2009 to April 2010) as well as assessing its quality. A further purpose is to compare the SMILES measurements with the operational winds analysis by the European Centre for Medium-Range Weather Forecasts (ECMWF). At mid-latitude in the mid-stratosphere, ECMWF winds are expected to be reliable and to provide a good data set to check the SMILES wind quality. On the other hand, ECMWF results are uncertain in the mid- and high stratosphere of the tropical region. Because of the lack of other stratospheric wind measurements, SMILES data offer a unique opportunity to estimate the performances of the ECMWF wind analyses in this region.

In Sect. 2, we briefly describe the measurement method. The theoretical precision (random errors) and accuracy (systematic errors) are estimated from a sensitivity study. Section 3 assesses the quality of the SMILES data by checking the internal consistency of the different SMILES products. The mean differences with the ECMWF winds are discussed. Results are illustrated with monthly global maps and the daily variation of the zonal-winds in Sect. 4. Both the measured Semi-Annual Oscillations (SAO) of the zonal-wind above the Equator, and the zonal-wind reversals between 50° N– 55° N during Arctic Sudden Stratospheric Warming (SSW) events are discussed and

are compared with the ECMWF analysis. Finally, we summarise our results and give conclusions as well as discuss ongoing work for improving the SMILES wind products.

2 SMILES observations

2.1 Measurement method

5 SMILES was attached to the ISS in Sept 2009 and functioned for 7 months until April 2010. It observed the Earth's limb, scanning from -7 to 100 km in 53 s, providing 1600 spectral radiance profiles per day. Using superconductor-Insulator-superconductor (SIS) detectors cooled at 4 K, it provided high quality spectra allowing constituent profiles of many species such as ozone (O_3) and hydrogen chloride (HCl) to
10 be derived (Kasai et al., 2006; Takahashi et al., 2010; Khosravi et al., 2012). SMILES observed spectral lines from the atmospheric limb in three frequency bands, named A (624.3 – 625.5 GHz), B (625.1 – 626.3 GHz) and C (649.1 – 650.3 GHz) but only two are measured simultaneously. Two acousto-optical spectrometers (AOS-1 and AOS-2) with similar specifications are used. Frequency calibration and stability are ensured using
15 an ultra-stable oscillator and frequent comb calibration of the AOS (Mizobuchi et al., 2012). Inherent in the spectra is information on the Doppler shift caused by the ISS (~ 4 km s $^{-1}$ along the line of sight) as well as atmospheric motion. The broadening of the spectral lines into several spectral channels provides enough sensitivity to detect the small frequency shift induced by the winds (e.g. a 50 ms $^{-1}$ line-of-sight wind
20 induced a shift of 100 kHz which has to be compared to the spectrometer spectral resolution of 1.2 MHz). For deriving wind, the two strongest spectral lines have been used separately. One is an emission line of O_3 at 625.371 GHz common to bands A and B, and the second one is a $H^{35}Cl$ triplet at 625.92 GHz (band B). Hence, three winds profiles are independently retrieved, two from the O_3 line in bands A and B, and one from
25 the HCl triplet in band B. The wind retrieval algorithm is similar to the one presented in Baron et al. (2011) for the temperature and trace gas profiles retrieval (see Appendix for

SMILES winds

P. Baron et al.

Title Page

Abstract

Introduction

Conclusions

References

Tables

Figures

◀

▶

◀

▶

Back

Close

Full Screen / Esc

Printer-friendly Version

Interactive Discussion



more details). The retrieved wind profiles are corrected to take into account the altitude dependence of the line-of-sight velocity which is neglected in the trace gas retrieval algorithms ($\sim 0.8 \text{ m s}^{-1} \text{ km}^{-1}$).

Because of the geometry of the instrument field of view in relation to the ISS orbit, the meridional component ($\pm 10^\circ$) of the wind is measured on the ascending portion of the orbit while the zonal component is measured on the descending portion. Figure 2 shows single line-of-sight wind retrievals at 36 km on 2 and 26 January for both ascending and descending portions of the orbits. Winds are retrieved near the meridional or the zonal directions between $\sim 30^\circ \text{ S}$ to $\sim 55^\circ \text{ N}$. The full latitude range of observations is between 38° S and 65° N but on the borders, the line-of-sight rotates quickly and deviates from the meridional or zonal direction. Another characteristic of the observations is, as the result of the 2-months periodic local-time precession of the ISS, semi and diurnal variations of mesospheric winds such as those induced by tides should have been captured in the observations.

2.2 Theoretical estimation of the retrieval errors

Figure 3 (left panel) shows the vertical resolution of the retrieved wind profiles and the measurement responses that indicate the altitudes of good measurement sensitivity (Merino et al., 2002). Considering altitudes where the measurement response is between 0.9–1.1, a good sensitivity is found from 25 to 70 km (20–0.05 hPa) and from 25 to 80 km (20–0.01 hPa) for the O_3 and HCl line retrievals, respectively. According to the vertical resolution of the retrieved profiles, the best information is obtained from the O_3 line below 60 km (0.2 hPa), and from the HCl lines at altitudes above. The vertical resolution of the composite retrieved profile is 5–7 km up to 70 km and increases to 10 km at 80 km. Since the wind information comes from a layer of 5 to 10 km thickness around the line-of-sight tangent point, the horizontal resolution along the line-of-sight is between 500 and 700 km.

The theoretical precision and accuracy for a single profile retrieval are shown in the central and right panels of Fig. 3, respectively. The methodology and the assumptions

SMILES winds

P. Baron et al.

Title Page

Abstract

Introduction

Conclusions

References

Tables

Figures

◀

▶

◀

▶

Back

Close

Full Screen / Esc

Printer-friendly Version

Interactive Discussion



SMILES winds

P. Baron et al.

[Title Page](#)[Abstract](#)[Introduction](#)[Conclusions](#)[References](#)[Tables](#)[Figures](#)[◀](#)[▶](#)[◀](#)[▶](#)[Back](#)[Close](#)[Full Screen / Esc](#)[Printer-friendly Version](#)[Interactive Discussion](#)

of the error analysis are given in Baron et al. (2011), except for the errors on the calibration parameters which include a correction for a non-linearity in the receiver (Ochiai et al., 2012a). Here an error of 20 % is assumed on the non-linear parameters. The retrieval precision is limited by the measurement noise and to a lesser extent by the uncertainties in the O₃ and HCl abundances. The theoretical precision is 4–10 ms⁻¹ between 35 and 60 km (O₃ line retrieval) and < 20 ms⁻¹ between 60 and 80 km (HCl line retrieval). The lower limit of accurate retrieval is set by systematic effects on the ozone line retrieval (dashed black line), in particular errors on the intensity calibration of the spectra.

In summary, although the retrieval sensitivity reaches down to 25 km, good quality wind profiles (accuracy < 5 ms⁻¹) are actually retrieved from 35 km (8 hPa). The upper limit of the retrieval is 80 km using the band-B HCl line.

2.3 Data selection and ECMWF wind pairing

In this analysis, retrieved winds with a measurement response smaller than 0.9 are rejected. The retrieval quality is estimated from the sum of the squares of the spectral fit residual (χ^2). Abnormally high values of the χ^2 before the retrieval indicate scans with potential disturbances in the field-of-view or in the pointing. High values of the χ^2 after the retrieval indicates bad measurement fit. Note that disturbed observations can be fitted effectively but with incorrect wind values. Hence it is important to test the χ^2 before and after the retrieval. For the O₃ line in band-A (band-B), retrievals with a normalized χ^2 larger than 40 (30) before the inversion or larger than 2 (1.5) after the inversion are rejected. For the HCl line in band-B, the χ^2 thresholds for rejection are 50 before inversion and 2.5 after inversion.

ECMWF operational analysis data were used starting with Integrated Forecasting system (IFS) cycle 35 release 3 in September 2009. A major operational upgrade occurred in the middle of the mission on 26 January 2010, when cycle 36 release 1 was introduced with an increase of the model resolution from T799 to T1279 from 25 km

to 16 km. To compare the measurements with the ECMWF analysis, the SMILES profiles are paired with the closest ECMWF profile in space and time. ECMWF analyses were extracted on a latitude-longitude grid of $0.5 \times 0.5^\circ$ and 4 times per day, which corresponds to coincidence criteria of 3 h and 0.25° . The profiles extend up to 0.01 hPa (~80 km) with a vertical resolution of about 1.5 km in the middle stratosphere. The component of the ECMWF winds parallel to the SMILES line-of-sight is computed with the vertical resolution degraded to that of the retrieved profiles based on the shape of the retrieval averaging kernels.

2.4 Zero-wind correction

Errors which are not significant for trace gas retrieval, have not been fully characterized properly and were not included in the error analysis described in Sect. 2.2. However, wind retrievals are sensitive to some of these errors such as the spectrometer frequency calibration, the main local-oscillator frequency, the line-of-sight velocity correction and knowledge of the spectroscopic line frequency. The systematic component of these errors is mitigated by subtracting a daily “zero-wind” profile consisting of the average of observations with a direction near the meridional direction ($\pm 10^\circ$) and located in the tropics ($\pm 20^\circ$ from the equator) where the actual flow is predominantly zonal. Note that the latitude range of $\pm 20^\circ$ has been defined to minimize the atmospheric contribution in the zero-wind based on estimations using the ECMWF winds. Figure 4 shows the zero-winds at 50 km derived from the three SMILES products. At this altitude, the three products are retrieved with a good sensitivity and the spectrometer frequency error is expected to be the main measurement bias. For lines in band-B, which is always measured with the second spectrometer unit (AOS-2), the zero-wind corrections vary between 20–40 ms^{-1} and the day-to-day changes do not exceed 5 ms^{-1} . The zero-wind correction retrieved from the O_3 line in band-A shows two regimes depending which spectrometer is used. When the first spectrometer unit (AOS-1) is used for the measurements (configuration for measuring band-B simultaneously), the zero-wind correction values are between 50–70 ms^{-1} . When band-A is measured with AOS-2, the

Title Page

Abstract

Introduction

Conclusions

References

Tables

Figures

◀

▶

◀

▶

Back

Close

Full Screen / Esc

Printer-friendly Version

Interactive Discussion



SMILES winds

P. Baron et al.

[Title Page](#)[Abstract](#)[Introduction](#)[Conclusions](#)[References](#)[Tables](#)[Figures](#)[◀](#)[▶](#)[◀](#)[▶](#)[Back](#)[Close](#)[Full Screen / Esc](#)[Printer-friendly Version](#)[Interactive Discussion](#)

zero-wind values are similar to those obtained for band-B. After removing the atmospheric wind variability estimated using ECMWF winds (ECMWF zero-wind in Fig. 4), a linear trend of $\sim 20 \text{ m s}^{-1}/6\text{-months}$ is seen on the 4 observational configurations (not shown). This trend is compatible with the main local-oscillator stability expected to be $\frac{\delta_\nu}{\nu} = 6.8 \times 10^{-8}/6\text{-months}$ where ν is the local oscillator frequency. Zero-wind corrections relevant to band B oscillate with a period of 2-months and an amplitude of $10\text{--}20 \text{ m s}^{-1}$. Although the period is compatible with that of the instrument thermal variation, the origin of the oscillation on the band-B zero-wind is not yet fully understood.

Such frequency offsets ($< 0.1 \text{ MHz}$) are acceptable for trace gas retrievals which are the first objective of the mission. However it is clearly not good enough for wind retrieval which requires the “zero-wind” correction. However, as seen by the ECMWF zero-wind, during some periods between December and February the atmospheric contribution in the zero-wind correction can reach $\sim 10 \text{ m s}^{-1}$ which would introduce a bias in the wind profile if solely corrected with the retrieved zero-wind value. In order to reduce this bias, the subtraction of the retrieved zero-wind is compensated by the addition of ECMWF zero-wind. Above 0.01 hPa , ECMWF winds are not available and are linearly extrapolated.

3 Data quality assessment and comparison with ECMWF analysis

The data quality assessment consists, first, of checking the internal consistency of the SMILES data since winds are derived from different spectroscopic lines and spectrometers. For further verification, retrieved winds need to be compared with independent wind information. Lacking other measurements in the middle and upper stratosphere, such information is taken from the operational ECMWF analyses. It is known that, at high altitudes, tropical ECMWF winds are poorly constrained. Baldwin and Gray (2005) have compared ECMWF ERA-40 reanalysis zonal-winds with observations from two tropical stations. They found good agreement below $2\text{--}3 \text{ hPa}$ but, at higher altitudes, their conclusion was that the reanalysis winds should be used with caution (correlation

of 0.3 at 0.1 hPa with observations). Hence, the comparison of SMILES with ECMWF winds is not only relevant for the SMILES wind quality assessment but it also provides insights on the quality of the ECMWF winds themselves. For full verification of the SMILES winds, the mesospheric measurements should also be validated with ground-based radar observations. However such analysis is beyond the scope of this paper.

3.1 Internal consistency check

The upper panels of Fig. 5 show the mean meridional wind profiles in 20° latitude bins between 20° S and 60° N that have been retrieved from the O₃ lines in bands A and B (blue and green lines, respectively) and from the HCl line in band B (red line). Only measurements when bands A and B were measured simultaneously are used. The retrieved winds have been corrected with the zero-wind profile.

Between 4 and 0.1 hPa, good agreement is found for winds retrieved from the O₃ lines in all latitude bands. The standard deviation of the retrieved winds (Fig. 5, lower panels) also confirms the good agreement between the O₃ retrievals in this altitude range. At lower (8–4 hPa) and upper (< 0.1 hPa) altitudes, O₃ line derived winds exhibit differences that reach ~ 10 ms⁻¹ at higher latitudes.

As indicated in Sect. 2.2, in the upper retrieval range (0.1–0.01 hPa), winds retrieved from the HCl line should be preferred. Between 1 and 0.1 hPa, the mean and the standard deviation of the profiles retrieved from the HCl line (dashed-red line) match those from the O₃ retrievals. At higher altitudes, the mean and standard deviation of the HCl wind profiles smoothly expands up to 0.005 hPa. In the lower part of the retrieval range (> 1 hPa), large differences with O₃ retrievals can be seen as expected from the degradation of the accuracy and the precision of the HCl line retrieval.

The left panel of Fig. 6 shows the differences between profiles retrieved from the O₃ and the HCl lines in band-B between 40 and 70 km. At 50 and 60 km, the standard deviation and the mean of the differences are 12 ms⁻¹ and < 1.2 ms⁻¹, respectively. Since both profiles are derived from simultaneous measurements with the same spectrometer, the standard deviation is representative of the errors due to the measurement

SMILES winds

P. Baron et al.

Title Page

Abstract

Introduction

Conclusions

References

Tables

Figures

◀

▶

◀

▶

Back

Close

Full Screen / Esc

Printer-friendly Version

Interactive Discussion



thermal noise. The value is consistent with the theoretical estimate: $5\text{--}8\text{ ms}^{-1}$ and 10 ms^{-1} for O_3 and HCl retrievals, respectively. At 70 km, the standard deviation increases to 16 ms^{-1} which is also consistent with the loss of precision for both O_3 and HCl retrievals (20 ms^{-1} and 13 ms^{-1} , respectively). The slight overestimation of the O_3 -line retrieval precision is because of the large variability of the mesospheric O_3 line intensity in the mesosphere.

The comparison of the winds derived from the ozone line simultaneously measured in bands A and B (different spectrometers) and corrected with the zero-wind technique is shown in Fig. 6 (right panel). The mean difference at altitudes between 40–60 km is less than 3 ms^{-1} and the standard deviation of the differences is 7 ms^{-1} . At 30 km, the mean difference and the standard deviation increase to 6 ms^{-1} and 13 ms^{-1} , respectively. Since the profiles are retrieved from the same spectral line, the measurement thermal noise is correlated at more than 90% and the differences between the retrievals arise from errors on the spectrometer channels frequency. We checked that the difference is random from one retrieval to another. Hence, the residual errors from the spectrometer channels frequency after the zero wind correction can be assumed as a random retrieval error of $\sim 5\text{--}7\text{ ms}^{-1}$.

In conclusion, the different SMILES products agree with each other in the mid- and upper stratosphere where the retrieval performances are similar for each product. Our results also confirm that winds retrieved from the O_3 line should be used between 8–0.1 hPa while those obtained from the HCl line retrievals should be used between 0.1–0.01 hPa. The theoretical estimate of the retrieval precision is underestimated by 5 ms^{-1} due to a residual error after the zero-wind correction. The additional noise likely arises from the fluctuation in the spectrometer frequency errors. Taking into account this additional noise, the total precision of the wind retrieval becomes $7\text{--}9\text{ ms}^{-1}$ in the middle and upper stratosphere.

SMILES winds

P. Baron et al.

[Title Page](#)[Abstract](#)[Introduction](#)[Conclusions](#)[References](#)[Tables](#)[Figures](#)[◀](#)[▶](#)[◀](#)[▶](#)[Back](#)[Close](#)[Full Screen / Esc](#)[Printer-friendly Version](#)[Interactive Discussion](#)

3.2 Comparison with the ECMWF meridional component

The internal checks presented in the previous section do not allow us to estimate the impacts of errors of the platform line-of-sight velocity, and of the local-oscillator frequency, which affect the three wind products in the same way. However in the tropics and extra-tropical stratosphere where meridional velocities are weak (Fig. 5), the differences between ECMWF and SMILES single profiles are caused by the retrieval errors, and, to a lesser extent, by non-coincident and non-simultaneous profile pairing and by uncertainties of ECMWF analysis. Hence the analysis of the differences between SMILES and ECMWF meridional winds in the stratosphere allows us to verify the wind retrieval error estimations.

The mean and the standard deviation of the differences (SMILES-ECMWF) have been calculated in latitude bins of 5° for data between November 2009 and April 2010, and with a line-of-sight within $\pm 10^\circ$ around the meridional direction. We rejected the days when less than 10 profiles were used to construct the zero-wind profile. Fig. 7 (lower panels) shows the results for the data retrieved from the O_3 line in band B. Over most of the region between 5–0.5 hPa, the bias between the model and the measurement (left panel) is less than 2 ms^{-1} and the standard deviation (right panel) is less than 10 ms^{-1} . However, the bias in the tropics is not relevant since the zero-wind correction is scaled according to the mean ECMWF tropical meridional wind. According to these results, the precision (standard deviation) and the accuracy (bias) for a single retrieved profile cannot exceed 10 ms^{-1} and 2 ms^{-1} , respectively, which is consistent with the error estimation.

At high latitudes (40° N – 60° N), a mean difference of 2 – 5 ms^{-1} is found at 4–3 hPa which may arise from the increase of the measurement bias and also from the larger variability of the meridional winds (Fig. 5). At lower altitudes ($> 8 \text{ hPa}$) and outside the tropics, the large mean differences are due to measurement calibration errors. The calibration errors are found to be larger for the O_3 line band-A retrieval (not shown). In the mesosphere, above 0.3 hPa, results from the O_3 and the HCl lines (upper panels)

Title Page

Abstract

Introduction

Conclusions

References

Tables

Figures



Back

Close

Full Screen / Esc

Printer-friendly Version

Interactive Discussion



look very similar and are consistent with the decrease of the estimated measurement precision (between 13 and 20 ms⁻¹). The mean differences in the mesosphere vary between -5 and 10 ms⁻¹.

3.3 Comparison with the ECMWF zonal component

5 In Fig. 8, the same methodology as the previous section is applied for deriving the mean and standard deviation of differences between SMILES (band-B) and ECMWF zonal ($\pm 10^\circ$) winds. Zonal winds are in general significantly larger than the meridional ones, and thus, the results are more sensitive to mismatches due to profile pairing and ECMWF uncertainties.

10 As for the meridional component, large mean differences, likely due to intensity calibration errors, are found at lower altitudes (> 8 hPa) in the extra-tropical regions (lower right panel) and at latitudes $< 30^\circ$ S because of the fast rotation of the line-of-sight from the zonal to meridional direction. However in most of the stratosphere (4–1 hPa), a low bias < 2 ms⁻¹ is found except over the Equator where the mean difference is between 5–10 ms⁻¹. In the mesosphere (1–0.01 hPa, upper right panel), a large positive difference (20–30 ms⁻¹) is found in the tropics and a negative difference at higher northern latitudes (between -20 and -10 ms⁻¹).

15 The standard deviations from the middle-stratosphere to lower mesosphere (lower right panel) are slightly higher than the values found for the meridional components. Such an increase of the standard deviation is consistent with the increase of uncertainties in profile-pairing and in ECMWF winds. However, values below 10 ms⁻¹ are still found over wide regions and more particularly in the extra-tropics indicating that SMILES captured the large variations of the zonal winds (-70 to +70 ms⁻¹) with a precision which is consistent with the estimation of 7–9 ms⁻¹. In the tropical mesosphere (0.1–0.01 hPa, upper panels), the standard deviation is between 15 and 20 ms⁻¹ which also corresponds to the retrieval precision. At northern mid-latitudes, the mesospheric standard deviation significantly increases to 20–30 ms⁻¹, likely due to the increase of errors in profile-pairing and of the ECMWF analysis itself.

SMILES winds

P. Baron et al.

Title Page

Abstract

Introduction

Conclusions

References

Tables

Figures



Back

Close

Full Screen / Esc

Printer-friendly Version

Interactive Discussion



The comparisons of the meridional and zonal winds derived from SMILES with those from ECMWF are a further indication of the quality of the measurements and of the retrieval process. The large differences in the zonal-winds found in the tropics and in the mesosphere indicate that SMILES observations have enough sensitivity to improve the ECMWF zonal wind analyses where the geostrophic approximation is not satisfied.

4 Examples of the observed wind fields

4.1 Monthly variation of zonal-winds

Figure 9 shows the zonally and monthly averaged zonal-winds obtained from band-B between 30° S–55° N and from mid-October to mid-April. Information at lower altitudes > 0.1 hPa (< 65 km) is retrieved from the O₃ line and that for the upper altitudes is from the HCl triplet. Until the first week of November, ECMWF were not available to us and the zero-wind correction has been calculated with winds from the version 5.2 of the analysis of the Goddard Earth Observing System Data Assimilation System model (GEOS-5.2) (Reinecker, 2008). In November and February, the observation range expands poleward in the Southern Hemisphere because of the 180°-maneuver of the ISS when hosting the space shuttle. The space shuttle also docked in April, but the viewing geometry did not allow the construction of “zero-wind” profiles. Since the Southern Hemisphere observations corresponded only to a few days, it has been decided to only focus on the region observed in the normal operation mode (30° S–55° N).

The monthly climatology exhibits the main and well known characteristics of the seasonal variations of the zonal-winds. Near the equinoxes (October, March and April), in the stratosphere and the lower mesosphere, zonal-winds are primarily eastward. In December and January, they become stronger with a large inter-hemispheric contrast: eastward in the winter-time Northern Hemisphere and westward in the summer-time Southern Hemisphere.

Title Page

Abstract

Introduction

Conclusions

References

Tables

Figures

◀

▶

◀

▶

Back

Close

Full Screen / Esc

Printer-friendly Version

Interactive Discussion



SMILES winds

P. Baron et al.

[Title Page](#)[Abstract](#)[Introduction](#)[Conclusions](#)[References](#)[Tables](#)[Figures](#)[◀](#)[▶](#)[◀](#)[▶](#)[Back](#)[Close](#)[Full Screen / Esc](#)[Printer-friendly Version](#)[Interactive Discussion](#)

In the tropical upper-stratosphere and mesosphere (< 3 hPa), the main characteristics of the Semi-Annual-Oscillation (SAO) in the zonal-winds are seen with, in particular, the opposite phase between the stratosphere (westward in December) and the mesosphere (eastward in December). At lower altitudes (> 4 hPa), the SAO signal vanishes and is dominated by the the Quasi-Biennial Oscillation (QBO) which is in an easterly phase (westward winds) during that period. The observed tropical SAO is discussed in more details in Sect. 4.3.

Though the Arctic region is not observed by SMILES, the zonal winds in the northernmost mid-latitudes (45° N– 55° N) are influenced by the Arctic polar vortex (high westerlies) whose the southerly extent increases with altitude up to the stratopause (~ 1 hPa), e.g. in December and January. The dynamics of the Arctic winter 2009/2010 have been described in several studies (Wang and Chen, 2010; Dörnbrack et al., 2012; Kuttippurath and Nikulin, 2012). In early winter, planetary wave activity prevented the formation of a strong vortex in the lower stratosphere and the vortex eventually split at the beginning of December (minor stratospheric warming). From December onward, the vortex became strong throughout the stratosphere until a major sudden stratospheric warming (SSW) occurred on 24–26 January 2010. After this event, a weak vortex reformed and disappeared in April. It is shown in Sect. 4.2 that the effects of the two SSW are observed at 2 hPa in the daily variation of the mean zonal-wind between 50° N and 55° N. Hence, SMILES offers direct wind measurements for studying the SSW development from the mid-stratosphere (8 hPa) to the mesosphere as well as the interactions with the mid-latitudes.

4.2 The sudden stratospheric warming events

The effects of the major SSW at ~ 5 hPa (~ 36 km) are clearly seen in Fig. 2. The coloured background indicates the abundance of N_2O from a dynamical model driven by ECMWF winds on the 850 K surface and constrained by Odin/SMR observations (Rösevall et al., 2007). The polar vortex is characterised by low values of N_2O (blueish colour) inside and high values (yellow colour) on its border. On 2 January

2010, the vortex is well centered above the polar region and strong eastward winds are measured on its periphery. The direction of the meridional component is alternatively southward or northward following the vortex meanders. On 26 January, the vortex is displaced over the North of Europe and it is confined between 60° W and 120° E. Inside the vortex, SMILES observed the change of the direction of the meridional winds due to the counterclockwise rotation of the flow. Outside the vortex a westward flow is measured due to an anti-cyclonic system located above the pacific.

Figure 10 (red dots) shows the daily variation at ~2 hPa of zonally averaged zonal-winds measured between 50° N–55° N. The time series is made from the O₃ line retrievals. When both bands A and B are measured simultaneously, only band-B is used. The error bars correspond to the daily-mean precision \bar{e} ($2\text{-}\sigma$):

$$\bar{e} = \sqrt{\frac{e^2}{n_{\text{zero}}} + \frac{e^2 + e_s^2}{n_{\text{wind}}}}, \quad (1)$$

where $e = 5 \text{ ms}^{-1}$ is the single profile retrieval precision at 2 hPa (Sect. 2.2), $e_s = 5 \text{ ms}^{-1}$ is the additional noise arising from the zero-wind correction (Sect. 3.1) and, n_{zero} and n_{wind} are the number of profiles to construct the daily zero-wind and the mean zonal-wind, respectively. The first term below the root-square operator is added to account for the retrieval errors on the zero-wind profiles.

A minor and a major SSW occurred in the beginning of December and at the end of January, respectively. In both cases, a reversal of the mean zonal flow direction is measured between 50° N–55° N, accompanied by a steep increase of the temperature in the Arctic (blue dashed line). The temperature data are daily and zonally averaged AURA/MLS observations (Schwartz et al., 2008; Limpasuvan et al., 2005) between 60° N–80° N. The wind and temperature observations are consistent with the analysis of meteorological data in the Arctic of various winters (Labitzke and Kunze, 2009; Manney et al., 2009; Dörnbrack et al., 2012). In the beginning of January, when the vortex had the strongest intensity, the mean eastward zonal-winds strongly increased

SMILES winds

P. Baron et al.

Title Page	
Abstract	Introduction
Conclusions	References
Tables	Figures
◀	▶
◀	▶
Back	Close
Full Screen / Esc	
Printer-friendly Version	
Interactive Discussion	



to 60–80 ms⁻¹. Then, the flow direction gradually changed until the end of January (–20 ms⁻¹). The flow returned to a normal eastward direction in few days and reached a maximum velocity of 40 ms⁻¹ in the beginning of March and decreased again when the vortex disappeared in the springtime.

The ECMWF zonal-winds (Fig. 10, black dots) are consistent with the measurements. A good agreement (difference < 5 ms⁻¹) is found on average. The largest differences (10–15 ms⁻¹) are found in beginning of November and January when the vortex was strongest.

4.3 Zonal wind development in the tropics

Figure 11 shows the daily-averaged zonal-wind over the equator ($\pm 5^\circ$) using the same averaging method as in Sect. 4.2. When band-B is measured, data above 0.1 hPa are replaced by the HCl line retrievals. The downward progression from the lower mesosphere to the middle stratosphere of the eastward phase (reddish colour) is typical of the winter SAO signal (Hirota, 1980; Garcia et al., 1997). A large variation amplitude is measured at the stratopause (~ 1 hPa) where a complete reversal of the wind direction occurred: +40 ms⁻¹ (eastward) in November, –60 ms⁻¹ in January and +40 ms⁻¹ in April. In the mesosphere (0.1–0.007 hPa), the data set, based on the HCl line measured in band-B, is quite sparse. It shows that the wind flow also varies over a large velocity range (between –60 and +60 ms⁻¹) but, as expected, the wind direction changes in anti-phase with the stratosphere (Hitchman et al., 1997; Lossow et al., 2008).

At lower altitudes (below 5 hPa), the SAO amplitude decreases and is mixed with the QBO (Hirota, 1980; Baldwin and Gray, 2005). The westward flow measured over most of the period below 5 hPa is consistent with the easterly (westward) phase phase of the QBO during the SMILES period. Unfortunately the time period observed is too short to see a full cycle of the QBO.

Figure 12 shows the comparison with ECMWF analysis of daily-averaged zonal-winds at 4, 2 and 0.2 hPa (35, 40, and 60 km) between 15° S–15° N. The error bars

Title Page

Abstract

Introduction

Conclusions

References

Tables

Figures

◀

▶

◀

▶

Back

Close

Full Screen / Esc

Printer-friendly Version

Interactive Discussion



SMILES winds

P. Baron et al.

[Title Page](#)[Abstract](#)[Introduction](#)[Conclusions](#)[References](#)[Tables](#)[Figures](#)[◀](#)[▶](#)[◀](#)[▶](#)[Back](#)[Close](#)[Full Screen / Esc](#)[Printer-friendly Version](#)[Interactive Discussion](#)

correspond to the precision of the daily-averaged profiles (see Sect. 4.2) assuming $e = 7, 5$ and 7 ms^{-1} and $e_s = 7, 5$ and 5 ms^{-1} for the three altitudes, respectively. Southern and northern tropics are shown separately in order to account for the asymmetry around the equator: Southern Hemisphere winds are shifted toward the westward direction and the amplitude of the wind variation is larger than that in the Northern Hemisphere. For instance at 2 hPa, winds vary between -60 and 30 ms^{-1} on the southern side of the equator and between -30 and 40 ms^{-1} on the northern side. Note that neither the SAO nor the QBO are responsible for the asymmetry since both are symmetric about the equator. Because of the increase of the SAO with altitude, the wind variation is larger in the upper-stratosphere (2 hPa) than in the mid-stratosphere (4 hPa).

In the stratosphere (4 and 2 hPa), the ECMWF analyses reproduce the measurements fairly well. However, at 2 hPa, the variation range is larger in the measurements by $20\text{--}30 \text{ ms}^{-1}$. In particular, the strong increase of the westward zonal-winds measured during the two first weeks of February in both hemispheres is not seen in the ECMWF analyses. On the contrary, at this time, the ECMWF winds start the westward-to-eastward flow transition. Daily and zonally averaged MLS temperatures for the same latitude range are shown along with the winds. The signature of the SAO in the temperature is in phase with the winds SAO: warmer temperature during the eastward flow and cooler temperature during the westward flow. Note that the transition from the cooler to warmer temperature starts ahead (end of January) compared to the measured westward-to-eastward transition of the zonal winds (beginning of February). It is during this period that the large mismatch between SMILES and ECMWF winds occurs.

In the lower mesosphere (0.2 hPa), the measured wind SAO is in phase with the stratospheric oscillation but its amplitude is much smaller ($\sim 20 \text{ ms}^{-1}$). It is also in phase with the temperature oscillation, which has the opposite phase to that of the stratospheric temperature. The ECMWF winds depart significantly from SMILES winds by a constant offset of about 20 ms^{-1} (consistent with Fig. 8). However, the amplitude of the oscillation is consistent with the observed one. Day-to-day variations are more

pronounced in the measurements than in ECMWF winds. In particular, in the Northern Hemisphere, between November and January, the measurements exhibit an oscillation with a period of 10–20 days and an amplitude of $\sim 20 \text{ ms}^{-1}$ which is compatible with a quasi-16 days planetary wave (Lastovicka, 1997). Note that tidal oscillation is aliased with a period of one month (semi-diurnal oscillation) and two months (diurnal oscillation) because of the 2-months precession of the ISS. This must be taken into account for the analysis of the mesospheric wind seasonal variations.

5 Conclusions

We have reported measurements of winds between 8–0.01 hPa and $30^\circ \text{ S}–55^\circ \text{ N}$ during the northern winter 2009–2010. Three winds products were derived from spectroscopic measurements by the sub-mm wave limb sounder JEM/SMILES. The zonal and meridional components were retrieved from different parts of the orbit. The precision and the accuracy are $7–9 \text{ ms}^{-1}$ and 2 ms^{-1} between 8–0.5 hPa and $< 20 \text{ ms}^{-1}$ and $< 5 \text{ ms}^{-1}$ in the mesosphere. The vertical resolution is 5–7 km from the mid-stratosphere to the lower mesosphere and $< 20 \text{ km}$ elsewhere. To our knowledge, this is the first time that winds have been observed between 35–60 km from space. Internal comparisons show a good quantitative agreement between the different SMILES products. Good agreement is also found with the ECMWF analyses in most of the stratosphere except for the zonal-winds over the equator (mean difference of $5–10 \text{ ms}^{-1}$). In the mesosphere SMILES and ECMWF zonal-winds exhibit large differences $> 20 \text{ ms}^{-1}$, especially in the tropics. These results demonstrate that SMILES measurements have the potential to significantly improve the capability of atmospheric models to predict winds in the tropical mid- and upper stratosphere, and in the mesosphere in general.

In coming work SMILES mesospheric winds will be validated using ground-based radar observations. We also expect better retrievals thanks to improvements of the calibrated spectra (radiance and frequency) and of the inversion methodology (e.g. joint inversion of different bands). The aim is to reliably retrieve winds down to 20–25 km

Title Page

Abstract

Introduction

Conclusions

References

Tables

Figures

◀

▶

◀

▶

Back

Close

Full Screen / Esc

Printer-friendly Version

Interactive Discussion



which is the theoretical limit for the SMILES measurements. In the mesosphere, the number of retrieved profiles can be increased by the use of the $H^{37}Cl$ lines measured in band-A (weaker than the band-B $H^{35}Cl$ line) and by using the O_3 line signal enhanced during night time.

Although the SMILES instrument was not designed for wind measurement, the retrieval performances are close to those used in Lahoz et al. (2005) for stressing the importance of stratospheric wind measurements (error $< 5 \text{ ms}^{-1}$ between 25–40 km). This indicates that a carefully designed sub-mm wave radiometer, which is mature technology, has the potential to significantly improve the prediction of wind in atmospheric models and to fill the altitude gap in the stratospheric wind measurements. The optimal specifications and the performances for such instrument are under study.

Appendix A

Retrieval procedure

The wind retrieval uses the algorithms version 2.1.5 developed for retrieving temperature and gas profiles in the SMILES level-2 research chain developed in NICT (<http://smiles.nict.go.jp/pub/data/products.html>). They are based on the standard least-squares method constrained by an a priori knowledge of the retrieved parameters. A zero profile is used for the wind a priori. The line-of-sight wind information is derived in a two step process using the ozone and HCl lines available in the spectra. Firstly the atmospheric constituent profiles relevant for the spectral region are retrieved disregarding any spectral shifts due to the wind which has no impact on the results. Then the wind is retrieved on a 5 km vertical grid. The vertical sampling of the retrieval grid is consistent with the information content of the spectra. The two inversion processes use a spectral window of 500 MHz around the chosen molecular lines. The forward model has been modified to include the Doppler frequency shift induced by the air parcels velocity and to compute the wind weighting functions. The frequency shift induced by the

SMILES winds

P. Baron et al.

Title Page

Abstract

Introduction

Conclusions

References

Tables

Figures

◀

▶

◀

▶

Back

Close

Full Screen / Esc

Printer-friendly Version

Interactive Discussion



SMILES winds

P. Baron et al.

Title Page

Abstract

Introduction

Conclusions

References

Tables

Figures

◀

▶

◀

▶

Back

Close

Full Screen / Esc

Printer-friendly Version

Interactive Discussion



wind is included as a change of the spectroscopic lines frequency. The wind weighting functions are computed with a perturbation method for the derivation of the absorption coefficient and with an analytic derivation of a discrete form of the radiative transfer equation (Urban et al., 2004). The frequency dependence of the source function (the Planck function) is neglected and we assume horizontal winds along the full line-of-sight which is only true at the tangent point. Both approximations have a negligible impact on the retrieved velocities in the altitude range considered in the analysis.

Acknowledgements. The SMILES project is jointly led by the Japan Aerospace Exploration Agency (JAXA) and the National Institute of Information and Communications Technology (NICT, Japan). We acknowledge the European Centre for Medium Range Weather Forecasts (ECMWF) and the Global Modeling and Assimilation Office (GMAO) at NASA Goddard Space Flight Center for access to model results. DPM and JU would like to thank the Swedish National Space Board for support. PB would like to thank K. Muranaga, T. Haru and S. Usui from Systems Engineering Consultants Co. (SEC) for their important contributions to the SMILES project. PB would like to thank Yvan Orsolini for fruitful discussions.

References

- Alcaydé, D. and Fontanari, J.: Neutral temperature and winds from EISCAT CP-3 observations, *J. Atmos. Terr. Phys.*, 48, 931–947, 1986. 32477
- Alexander, M. J., Geller, M., McLandress, C., Polavarapu, S., Preusse, P., Sassi, F., Sato, K., Eckermann, S., Ern, M., Hertzog, A., Kawatani, Y., Pulido, M., Shaw, T. A., Sigmond, M., Vincent, R., and Watanabe, S.: Recent developments in gravity-wave effects in climate models and the global distribution of gravity-wave momentum flux from observations and models, *Q. J. Roy. Meteor. Soc.*, 136, 1103–1124, doi:10.1002/qj.637, 2010. 32476
- Baldwin, M. P. and Dunkerton, T. J.: Propagation of the Arctic oscillation from the stratosphere to the troposphere, *J. Geophys. Res.*, 104, 30937–30946, doi:10.1029/1999JD900445, 1999. 32476
- Baldwin, M. P. and Gray, L. J.: Tropical stratospheric zonal winds in ECMWF ERA-40 reanalysis, rocketsonde data, and rawinsonde data, *Geophys. Res. Lett.*, 32, L09806, doi:10.1029/2004GL022328, 2005. 32483, 32491

SMILES winds

P. Baron et al.

[Title Page](#)[Abstract](#)[Introduction](#)[Conclusions](#)[References](#)[Tables](#)[Figures](#)[◀](#)[▶](#)[◀](#)[▶](#)[Back](#)[Close](#)[Full Screen / Esc](#)[Printer-friendly Version](#)[Interactive Discussion](#)

- Baldwin, M., Thompson, D., Shuckburgh, E., Norton, W., and Gillett, N.: Weather from the stratosphere?, *Science*, 301, 317–318, 2003. 32476
- Baron, P., Urban, J., Sagawa, H., Möller, J., Murtagh, D. P., Mendrok, J., Dupuy, E., Sato, T. O., Ochiai, S., Suzuki, K., Manabe, T., Nishibori, T., Kikuchi, K., Sato, R., Takayanagi, M., Murayama, Y., Shiotani, M., and Kasai, Y.: The Level 2 research product algorithms for the Superconducting Submillimeter-Wave Limb-Emission Sounder (SMILES), *Atmos. Meas. Tech.*, 4, 2105–2124, doi:10.5194/amt-4-2105-2011, 2011. 32479, 32481
- Derber, J. and Bouttier, F.: A reformulation of the background error covariance in the ECMWF global data assimilation system, *Tellus A*, 51, 195–221, doi:10.1034/j.1600-0870.1999.t012-00003.x, 1999. 32476
- Dörnbrack, A., Pitts, M. C., Poole, L. R., Orsolini, Y. J., Nishii, K., and Nakamura, H.: The 2009–2010 Arctic stratospheric winter – general evolution, mountain waves and predictability of an operational weather forecast model, *Atmos. Chem. Phys.*, 12, 3659–3675, doi:10.5194/acp-12-3659-2012, 2012. 32489, 32490
- Garcia, R. R., Dunkerton, T. J., Lieberman, R. S., and Vincent, R. A.: Climatology of the semi-annual oscillation of the tropical middle atmosphere, *J. Geophys. Res.*, 102, 26019–26032, 1997. 32491
- Hamilton, K.: Dynamics of the tropical middle atmosphere: a tutorial review, *Atmos. Ocean*, 36, 319–354, 1998. 32476
- Hays, P. B., Abreu, V. J., Dobbs, M. E., Gell, D. A., Grassl, H. J., and Skinner, W. R.: The high-resolution doppler imager on the upper-atmosphere research satellite, *J. Geophys. Res.*, 98, 10713–10723, 1993. 32477
- Hildebrand, J., Baumgarten, G., Fiedler, J., Hoppe, U.-P., Kaifler, B., Lübken, F.-J., and Williams, B. P.: Combined wind measurements by two different lidar instruments in the Arctic middle atmosphere, *Atmos. Meas. Tech.*, 5, 2433–2445, doi:10.5194/amt-5-2433-2012, 2012. 32477
- Hirota, I.: Observational evidence of the semiannual oscillation in the tropical middle atmosphere: a review, *Pure Appl. Geophys.*, 118, 217–238, 1980. 32491
- Hitchman, M. H., Kudeki, E., Fritts, D. C., Kugi, J. M., Fawcett, C., Postel, G. A., Yao, C. Y., Ortland, D., Riggan, D., and Harvey, V. L.: Mean winds in the tropical stratosphere and mesosphere during January 1993, March 1994, and August 1994, *J. Geophys. Res.*, 102, 26033–26052, 1997. 32491

- Holton, J. R. and Alexander, M. J.: The role of waves in the transport circulation of the middle atmosphere, in: *Geophys. Monogr. Ser.*, vol. 123, AGU, Washington, DC, 21–35, 2000. 32476
- Jacobi, C., Arras, C., Kürschner, D., Singer, W., Hoffmann, P., and Keuer, D.: Comparison of mesopause region meteor radar winds, medium frequency radar winds and low frequency drifts over Germany, *Adv. Space Res.*, 43, 247–252, available at: <http://www.sciencedirect.com/science/article/pii/S0273117708003359>, 2009. 32477
- Kasai, Y. J., Urban, J., Takahashi, C., Hoshino, S., Takahashi, K., Inatani, J., Shiotani, M., and Masuko, H.: Stratospheric ozone isotope enrichment studied by submillimeter wave heterodyne radiometry: observation capabilities of SMILES, *IEEE T. Geosci. Remote*, 44, 676–693, 2006. 32479
- Khosravi, M., Baron, P., Urban, J., Froidevaux, L., Jonsson, A. I., Kasai, Y., Kuribayashi, K., Mitsuda, C., Murtagh, D. P., Sagawa, H., Santee, M. L., Sato, T. O., Shiotani, M., Suzuki, M., von Clarmann, T., Walker, K. A., and Wang, S.: Diurnal variation of stratospheric HOCl, ClO and HO₂ at the equator: comparison of 1-D model calculations with measurements of satellite instruments, *Atmos. Chem. Phys. Discuss.*, 12, 21065–21104, doi:10.5194/acpd-12-21065-2012, 2012. 32479
- Kikuchi, K., Nishibori, T., Ochiai, S., Ozeki, H., Irimajiri, Y., Kasai, Y., Koike, M., Manabe, T., Mizukoshi, K., Murayama, Y., Nagahama, T., Sano, T., Sato, R., Seta, M., Takahashi, C., Takayanagi, M., Masuko, H., Inatani, J., Suzuki, M., and Shiotani, M.: Overview and early results of the Superconducting Submillimeter-Wave Limb-Emission Sounder (SMILES), *J. Geophys. Res.*, 115, D23306, doi:10.1029/2010JD014379, 2010. 32478
- Killeen, T. L., Skinner, W. R., Johnson, R. M., Edmonson, C. J., Wu, Q., Niciejewski, R. J., Grassl, H. J., Gell, D. A., Hansen, P. E., Harvey, J. D., and Kafkalidis, J. F.: TIMED Doppler Interferometer (TIDI), optical spectroscopic techniques and instrumentation for atmospheric and space research III, *Proc. SPIE*, 3756, 289–301, doi:10.1117/12.366383, 1999. 32477
- Kuttippurath, J. and Nikulin, G.: A comparative study of the major sudden stratospheric warmings in the Arctic winters 2003/2004–2009/2010, *Atmos. Chem. Phys.*, 12, 8115–8129, doi:10.5194/acp-12-8115-2012, 2012. 32489
- Labitzke, K. and Kunze, M.: On the remarkable Arctic winter in 2008/2009, *J. Geophys. Res.*, 114, D00I02, doi:10.1029/2009JD012273, 2009. 32490
- Lahoz, W. A., Brugge, R., Jackson, D. R., Migliorini, S., Swinbank, R., Lary, D., and Lee, A.: An observing system simulation experiment to evaluate the scientific merit of wind and ozone

SMILES winds

P. Baron et al.

[Title Page](#)[Abstract](#)[Introduction](#)[Conclusions](#)[References](#)[Tables](#)[Figures](#)[◀](#)[▶](#)[◀](#)[▶](#)[Back](#)[Close](#)[Full Screen / Esc](#)[Printer-friendly Version](#)[Interactive Discussion](#)

SMILES winds

P. Baron et al.

[Title Page](#)[Abstract](#)[Introduction](#)[Conclusions](#)[References](#)[Tables](#)[Figures](#)[◀](#)[▶](#)[◀](#)[▶](#)[Back](#)[Close](#)[Full Screen / Esc](#)[Printer-friendly Version](#)[Interactive Discussion](#)

measurements from the future SWIFT instrument, Q. J. Roy. Meteor. Soc., 131, 503–523, 2005. 32494

Lastovicka, J.: Observations of tides and planetary waves in the atmosphere-ionosphere system, Adv. Space Res., 20, 1209–1222, doi:10.1016/S0273-1177(97)00774-6, 1997. 32493

5 Limpasuvan, V., Wu, D. L., Schwartz, M. J., Waters, J. W., Wu, Q., and Killeen, T. L.: The two-day wave in EOS MLS temperature and wind measurements during 2004–2005 winter, Geophys. Res. Lett., 32, L17809, doi:10.1029/2005GL023396, 2005. 32490

Lossow, S., Urban, J., Gumbel, J., Eriksson, P., and Murtagh, D.: Observations of the mesospheric semi-annual oscillation (MSAO) in water vapour by Odin/SMR, Atmos. Chem. Phys., 10, 6527–6540, doi:10.5194/acp-8-6527-2008, 2008. 32491

Maekawa, Y., Fukao, S., Yamamoto, M., Yamanaka, M. D., Tsuda, T., Kato, S., and Woodman, R. F.: First observation of the upper stratospheric vertical wind velocities using the Jicamarca VHF radar, Geophys. Res. Lett., 20, 2235–2238, doi:10.1029/93GL02606, 1993. 32477

15 Manney, G. L., Schwartz, M. J., Krüger, K., Santee, M. L., Pawson, S., Lee, J. N., Daffer, W. H., Fuller, R. A., and Livesey, N. J.: Aura Microwave Limb Sounder observations of dynamics and transport during the record-breaking 2009 Arctic stratospheric major warming, Geophys. Res. Lett., 36, L12815, doi:10.1029/2009GL038586, 2009. 32490

Marshall, A. G. and Scaife, A. A.: Impact of the QBO on surface winter climate, J. Geophys. Res., 114, D18110, doi:10.1029/2009JD011737, 2009. 32476

20 McDade, I. C., Shepherd, G. G., Gault, W. A., Rochon, Y. J., McLandress, C., Scott, A., Rowlands, N., and Buttner, G.: The stratospheric wind interferometer for transport studies (SWIFT), in: Igarss 2001: Scanning the Present and Resolving the Future, Vol. 3, Proceedings, 1344–1346, Sydney NSW, 9–13 July, doi:10.1109/IGARSS.2001.976839, 2001. 32477, 32502

25 Merino, F., Murtagh, D., Ridal, M., Eriksson, P., Baron, P., Ricaud, P., and de la Noe, J.: Studies for the Odin Sub-Millimetre Radiometer: III. Performance simulations, Can. J. Phys., 80, 357–373, doi:10.1139/P01-154, 2002. 32480

Mizobuchi, S., Kikuchi, K., Ochiai, S., Nishibori, T., Sano, T., Tamaki, K., and Ozeki, H.: In-orbit measurement of the AOS (Acousto-Optical Spectrometer) response using frequency comb signals, IEEE J. Sel. Top. Appl., 5, 977–983, doi:10.1109/JSTARS.2012.2196413, 2012. 32479

SMILES winds

P. Baron et al.

Title Page

Abstract

Introduction

Conclusions

References

Tables

Figures

◀

▶

◀

▶

Back

Close

Full Screen / Esc

Printer-friendly Version

Interactive Discussion



- Nezlin, Y., Rochon, Y., and Polavarapu, S.: Impact of tropospheric and stratospheric data assimilation on mesospheric prediction, *Tellus A*, 61, 154–159, doi:10.1111/j.1600-0870.2008.00368.x, 2009. 32476
- 5 Niciejewski, R., Wu, Q., Skinner, W., Gell, D., Cooper, M., Marshall, A., Killeen, T., Solomon, S., and Ortland, D.: TIMED Doppler interferometer on the Thermosphere Ionosphere Meso-
sphere Energetics and Dynamics satellite: data product overview, *J. Geophys. Res.-Space*, 111, A11S90, doi:10.1029/2005JA011513, 2006. 32477, 32502
- Ochiai, S., Kikuchi, K., Nishibori, T., and Manabe, T.: Gain nonlinearity calibration of submillimeter radiometer for JEM/SMILES, *IEEE J. Sel. Top. Appl.*, 5, 962–969, doi:10.1109/JSTARS.2012.2193559, 2012a. 32481
- 10 Ochiai, S., Kikuchi, K., Nishibori, T., Manabe, T., Ozeki, Hiroyuki Mizobuchi, S., and Iri-
majiri, Y.: Receiver performance of Superconducting Submillimeter-Wave Limb-Emission
Sounder (SMILES) on the international space station, *IEEE T. Geosci. Remote*, accepted, 2012b. 32478
- 15 Ortland, D. A., Skinner, W. R., Hays, P. B., Burrage, M. D., Lieberman, R. S., Marshall, A. R., and
Gell, D. A.: Measurements of stratospheric winds by the High Resolution Doppler Imager, *J. Geophys. Res.*, 101, 10351–10363, 1996. 32477, 32502
- Polavarapu, S., Shepherd, T. G., Rochon, Y., and Ren, S.: Some challenges of middle atmo-
sphere data assimilation, *Q. J. Roy. Meteor. Soc.*, 131, 3513–3527, doi:10.1256/qj.05.87,
20 http://dx.doi.org/10.1256/qj.05.87, 2005. 32476
- Reinecker, M.: The GEOS-5 data assimilation system: A documentation of GEOS-5.0, Tech
Report 104606 V27, NASA, 2008. 32488
- Rösevall, J. D., Murtagh, D. P., Urban, J., and Jones, A. K.: A study of polar ozone depletion
based on sequential assimilation of satellite data from the ENVISAT/MIPAS and Odin/SMR
25 instruments, *Atmos. Chem. Phys.*, 7, 899–911, doi:10.5194/acp-7-899-2007, 2007. 32489
- Rüfenacht, R., Kämpfer, N., and Murk, A.: First middle-atmospheric zonal wind profile mea-
surements with a new ground-based microwave Doppler-spectro-radiometer, *Atmos. Meas.
Tech.*, 5, 2647–2659, doi:10.5194/amt-5-2647-2012, 2012. 32477
- 30 Schwartz, M. J., Lambert, A., Manney, G. L., Read, W. G., Livesey, N. J., Froidevaux, L.,
Ao, C. O., Bernath, P. F., Boone, C. D., Cofield, R. E., Daffer, W. H., Drouin, B. J., Fet-
zer, E. J., Fuller, R. A., Jarnot, R. F., Jiang, J. H., Jiang, Y. B., Knosp, B. W., Krüger, K.,
Li, J.-L. F., Mlynczak, M. G., Pawson, S., Russell, J. M., I., Santee, M. L., Snyder, W. V.,
Stek, P. C., Thurstans, R. P., Tompkins, A. M., Wagner, P. A., Walker, K. A., Waters, J. W.,

SMILES winds

P. Baron et al.

[Title Page](#)[Abstract](#)[Introduction](#)[Conclusions](#)[References](#)[Tables](#)[Figures](#)[◀](#)[▶](#)[◀](#)[▶](#)[Back](#)[Close](#)[Full Screen / Esc](#)[Printer-friendly Version](#)[Interactive Discussion](#)

and Wu, D. L.: Validation of the Aura Microwave Limb Sounder temperature and geopotential height measurements, *J. Geophys. Res.*, 113, D15S11, doi:10.1029/2007JD008783, 2008. 32490

5 Shepherd, G. G., Thuillier, G., Gault, W. A., Solheim, B. H., Hersom, C., Alunni, J. M., Brun, J. F., Brune, S., Charlot, P., Cogger, L. L., Desaulniers, D. L., Evans, W. F. J., Gattinger, R. L., Girod, F., Harvie, D., Hum, R. H., Kendall, D. J. W., Llewellyn, E. J., Lowe, R. P., Ohrt, J., Pasternak, F., Peillet, O., Powell, I., Rochon, Y., Ward, W. E., Wiens, R. H., and Wimperis, J.: WINDII, The wind imaging interferometer on the upper-atmosphere research satellite, *J. Geophys. Res.*, 98, 10725–10750, 1993. 32477, 32502

10 Shepherd, T. G.: Transport in the middle atmosphere, *J. Meteorol. Soc. Jpn. II*, 85B, 165–191, 2007. 32476

Shepherd, T. G.: Dynamics, stratospheric ozone, and climate change, *Atmos. Ocean*, 46, 117–138, doi:10.3137/ao.460106, 2008. 32476

15 Sigmond, M., Scinocca, J. F., and Kushner, P. J.: Impact of the stratosphere on tropospheric climate change, *Geophys. Res. Lett.*, 35, L12706, doi:10.1029/2008GL033573, 2008. 32476

Stoffelen, A., Pailleux, J., Källén, E., Vaughan, J., Isaksen, L., Flamant, P., Wergén, W., Andersson, E., Schyberg, H., Culoma, A., Meynart, R., Endemann, M., and Ingmann, P.: The atmospheric dynamics mission for global wind field measurement, *B. Am. Meteorol. Soc.*, 86, 73–87, 2005. 32477, 32502

20 Swinbank, R. and Ortland, D. A.: Compilation of wind data for the Upper Atmosphere Research Satellite (UARS) Reference Atmosphere Project, *J. Geophys. Res.*, 108, 4615, 2003. 32477

Takahashi, C., Ochiai, S., and Suzuki, M.: Operational retrieval algorithms for JEM/SMILES level 2 data processing system, *J. Quant. Spectrosc. Ra.*, 111, 160–173, doi:10.1016/j.jqsrt.2009.06.005, 2010. 32479

25 Urban, J., Baron, P., Lautie, N., Schneider, N., Dassas, K., Ricaud, P., and De La Noe, J.: MOLIERE (v5): a versatile forward- and inversion model for the millimeter and sub-millimeter wavelength range, *J. Quant. Spectrosc. Ra.*, 83, 529–554, doi:10.1016/S0022-4073(03)00104-3, 2004. 32495

30 Wang, L. and Chen, W.: Downward Arctic Oscillation signal associated with moderate weak stratospheric polar vortex and the cold December 2009, *Geophys. Res. Lett.*, 37, L09707, doi:10.1029/2010GL042659, 2010. 32476, 32489

Wu, D. L., Schwartz, M. J., Waters, J. W., Limpasuvan, V., Wu, Q. A., and Killeen, T. L.: Mesospheric doppler wind measurements from Aura Microwave Limb Sounder (MLS), *Adv. Space Res.*, 42, 1246–1252, 2008. 32477, 32502

5 Žagar, N., Gustafsson, N., and Källén, E.: Variational data assimilation in the tropics: the impact of a background-error constraint, *Q. J. Roy. Meteor. Soc.*, 130, 103–125, doi:10.1256/qj.03.13, 2004. 32476

SMILES winds

P. Baron et al.

Title Page

Abstract

Introduction

Conclusions

References

Tables

Figures

◀

▶

◀

▶

Back

Close

Full Screen / Esc

Printer-friendly Version

Interactive Discussion



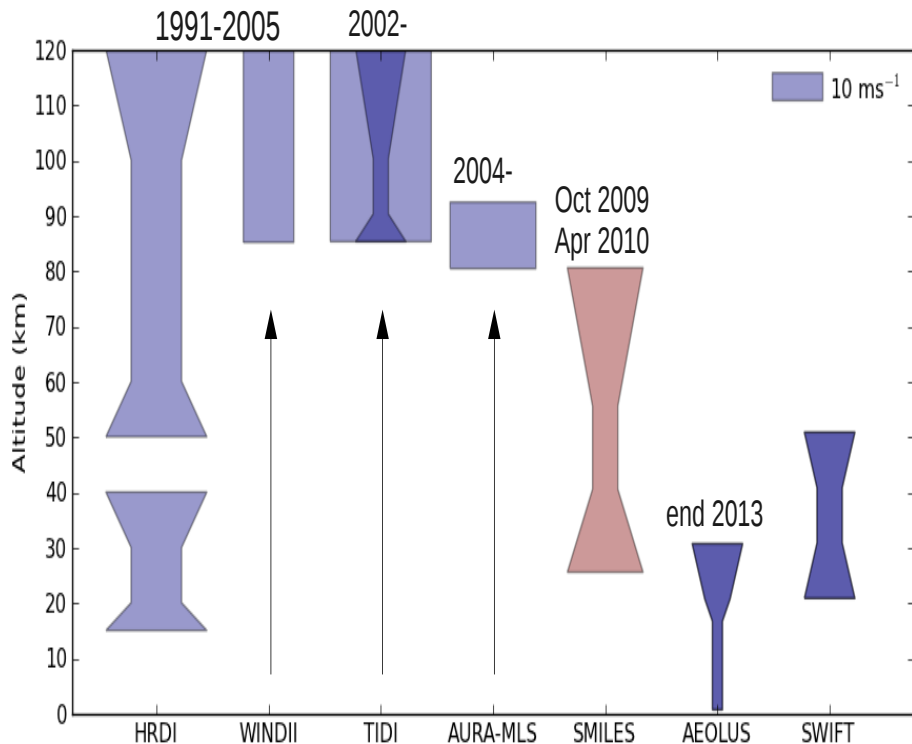


Fig. 1. The height coverage and estimated precision of past, current and future wind measuring instruments (reported validated precisions are indicated where possible, darker values are theoretical values). HRDI (Ortland et al., 1996) and WINDII (Shepherd et al., 1993) were on the UARS satellite and operated from September 1991–June 2005, TIDI (Niciejewski et al., 2006) operates on the TIMED satellite from 2002–present, AURA-MLS (Wu et al., 2008) operates on the AURA satellite from July 2004–present (note that wind is not a standard product), SMILES operated on the ISS from September 2009–April 2010, Aeolus is ESA mission (Stoffelen et al., 2005) planned for 2013 and SWIFT (McDade et al., 2001) is under study in Canada.

SMILES winds

P. Baron et al.

Title Page

Abstract	Introduction
Conclusions	References
Tables	Figures
◀	▶
◀	▶
Back	Close
Full Screen / Esc	
Printer-friendly Version	
Interactive Discussion	



SMILES winds

P. Baron et al.

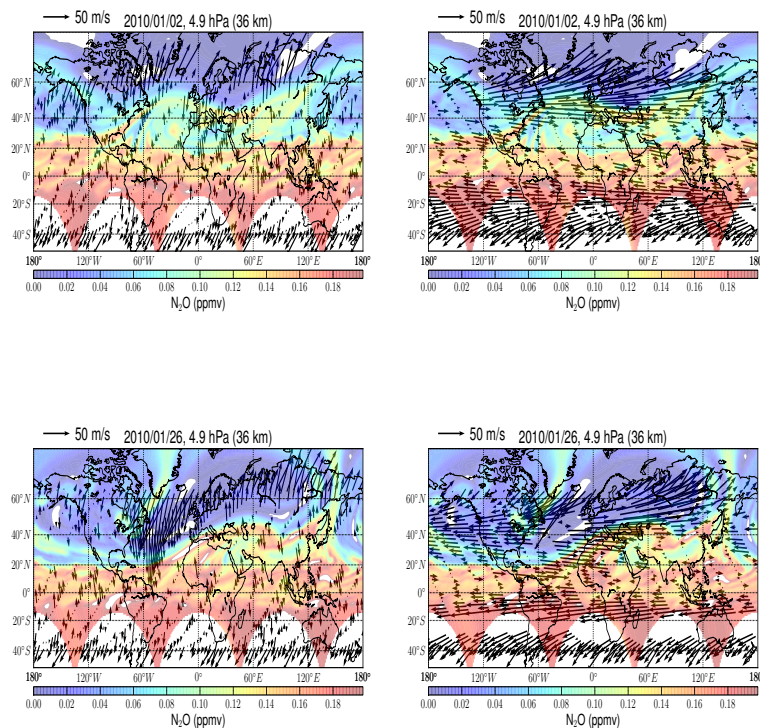


Fig. 2. Typical line-of-sight wind vectors retrieved at 5 hPa (~ 36 km) on 2 January 2010 (upper panels) and on 26 January 2010 (lower panels). The right panels correspond to the descending branch of the orbit where the meridional component of the wind is measured between $\sim 35^\circ$ S to $\sim 55^\circ$ N while the zonal component (left panels) is measured in the same latitude range on the ascending branch. The background colour shows the N_2O distribution from the assimilated Odin/SMR measurements in a model driven by ECMWF winds at the isentropic surface of 850 K.

[Title Page](#)
[Abstract](#)
[Introduction](#)
[Conclusions](#)
[References](#)
[Tables](#)
[Figures](#)
[◀](#)
[▶](#)
[◀](#)
[▶](#)
[Back](#)
[Close](#)
[Full Screen / Esc](#)
[Printer-friendly Version](#)
[Interactive Discussion](#)


SMILES winds

P. Baron et al.

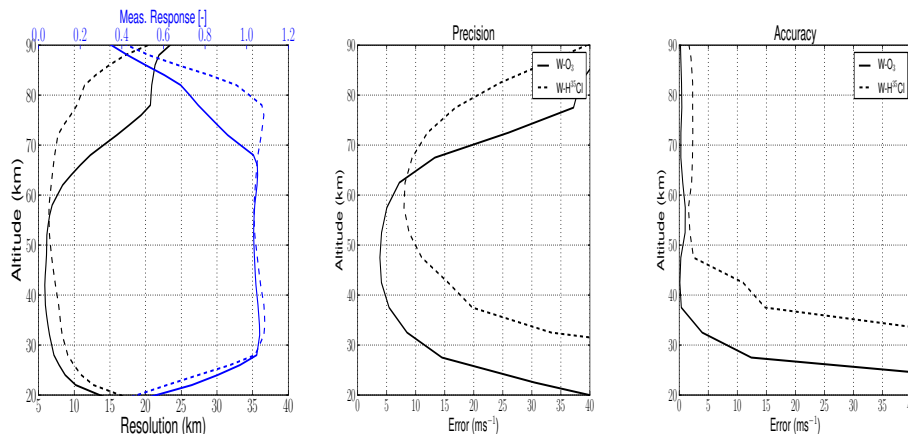


Fig. 3. Left panel: vertical resolution (dark line) and measurement response (blue line) for wind profiles retrieved from the O_3 spectral line (full lines) and from the H^{35}Cl triplets in band B (dashed lines). Central panel: estimates of wind retrieval precision derived from the O_3 spectral line (full line) and the H^{35}Cl triplets (dashed line). Right panel: same as central panel but for the accuracy.

SMILES winds

P. Baron et al.

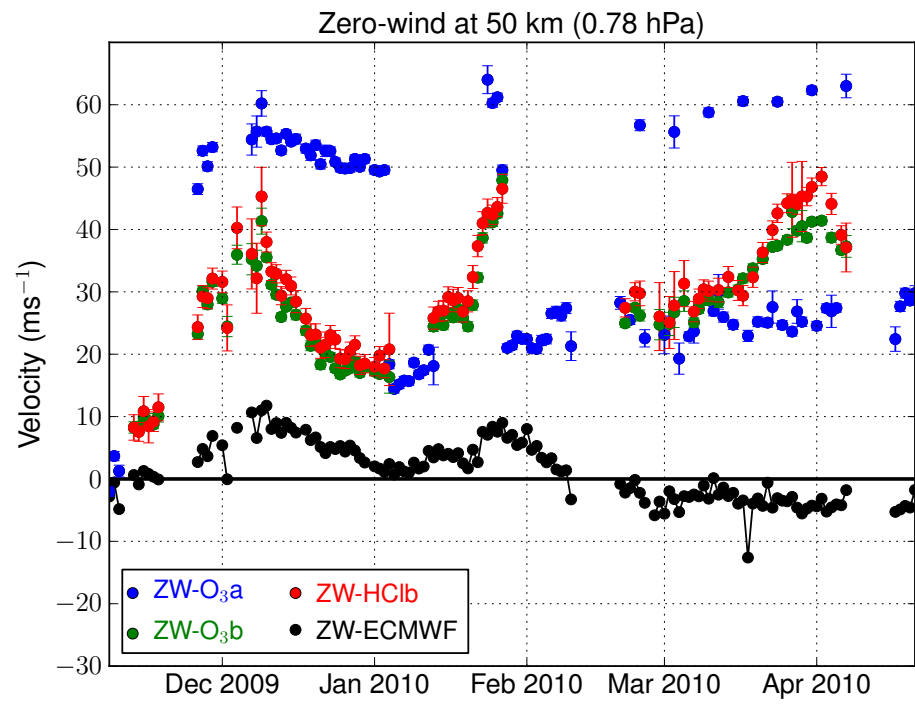


Fig. 4. Zero-wind for bias correction derived at 50 km from the O₃ line in band-A (blue dots), O₃ line in band-B (green dots) and HCl line in band-B (red dots) along with the zero-wind computed with the paired ECMWF winds.

Title Page

Abstract	Introduction
Conclusions	References
Tables	Figures

I ◀
▶ I

◀
▶

Back	Close
------	-------

Full Screen / Esc

Printer-friendly Version

Interactive Discussion



SMILES winds

P. Baron et al.

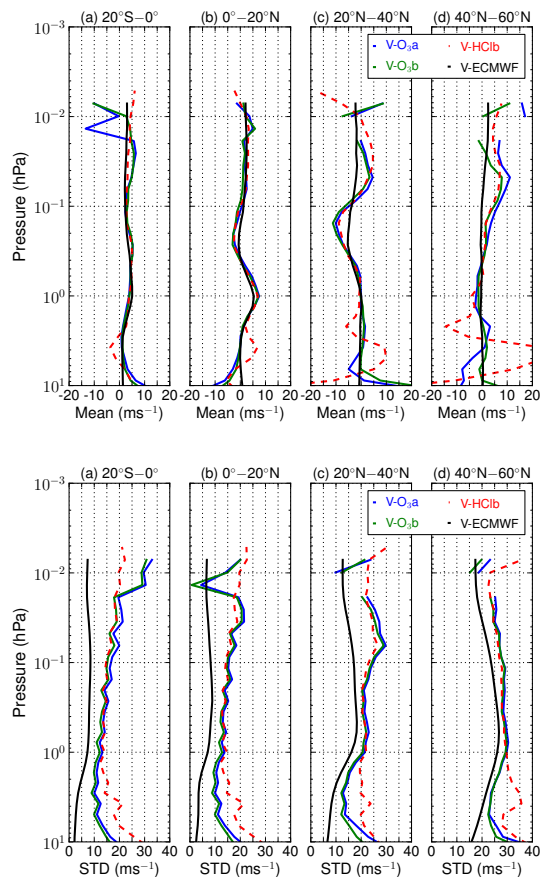


Fig. 5. Upper panels: zonally averaged meridional wind profiles retrieved from simultaneous measurements of the spectral lines: O₃-band A (blue line), O₃-band B (red line) and HCl-band B (green line). Lower panels: same as the upper panels but showing the standard deviation of the retrieved profiles. The results for the paired ECMWF profiles are also shown (black line).

[Title Page](#)
[Abstract](#)
[Introduction](#)
[Conclusions](#)
[References](#)
[Tables](#)
[Figures](#)
[◀](#)
[▶](#)
[◀](#)
[▶](#)
[Back](#)
[Close](#)
[Full Screen / Esc](#)
[Printer-friendly Version](#)
[Interactive Discussion](#)


SMILES winds

P. Baron et al.

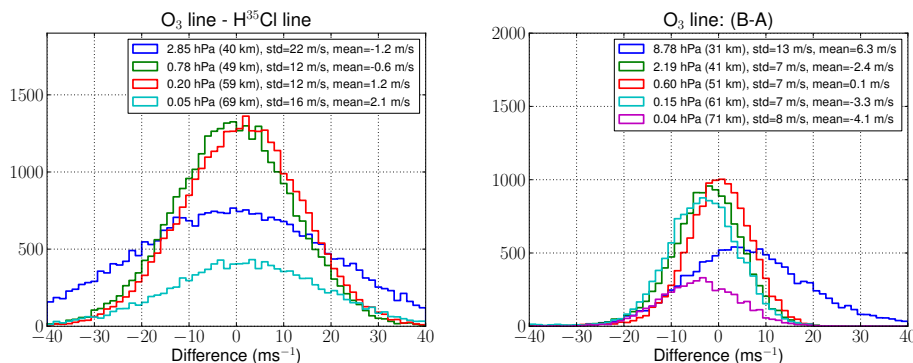


Fig. 6. Left panel: histogram of differences of the velocity retrieved from the O₃ and the HCl lines in band B. Right panel: same as for the left panel but for winds retrieved from the O₃ lines in bands A and B measured simultaneously. Data for latitudes between 20° N and 60° N have been used.

[Title Page](#)
[Abstract](#)
[Introduction](#)
[Conclusions](#)
[References](#)
[Tables](#)
[Figures](#)
[◀](#)
[▶](#)
[◀](#)
[▶](#)
[Back](#)
[Close](#)
[Full Screen / Esc](#)
[Printer-friendly Version](#)
[Interactive Discussion](#)


SMILES winds

P. Baron et al.

Title Page

Abstract

Introduction

Conclusions

References

Tables

Figures

◀

▶

◀

▶

Back

Close

Full Screen / Esc

Printer-friendly Version

Interactive Discussion

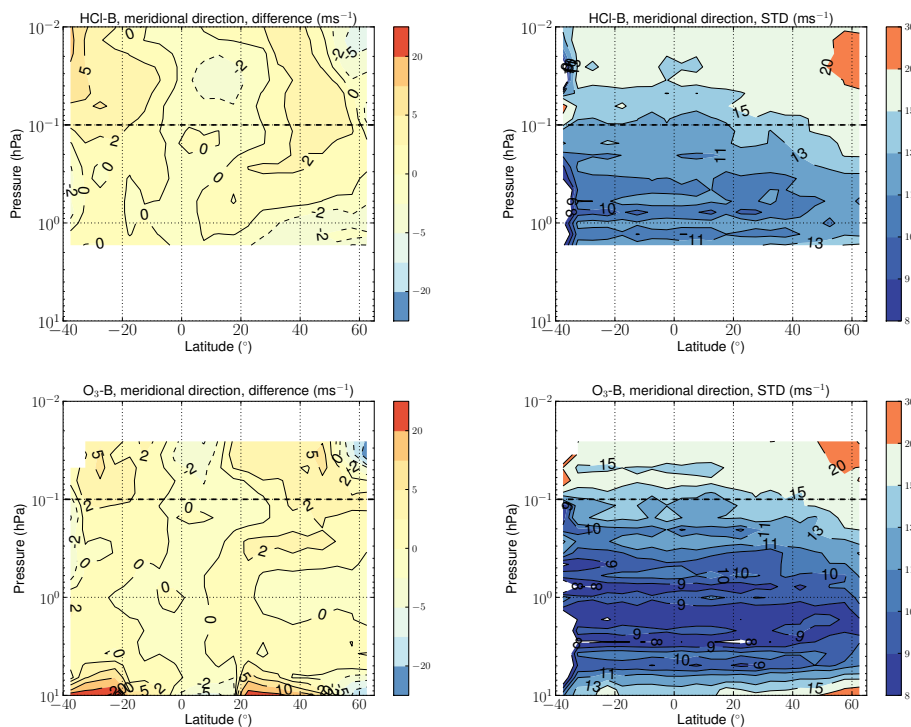


Fig. 7. Comparison of the meridional ($\pm 10^\circ$) winds retrieved from band-B with the operational ECMWF analyses. Upper panels: mean (left panel) and standard deviation (right panel) of the differences for profiles retrieved from the HCl lines. Lower panels: same as for the upper panels but for profiles retrieved from the O_3 line. Data between November 2009 to April 2010 have been selected.

SMILES winds

P. Baron et al.

Title Page

Abstract

Introduction

Conclusions

References

Tables

Figures



Back

Close

Full Screen / Esc

Printer-friendly Version

Interactive Discussion

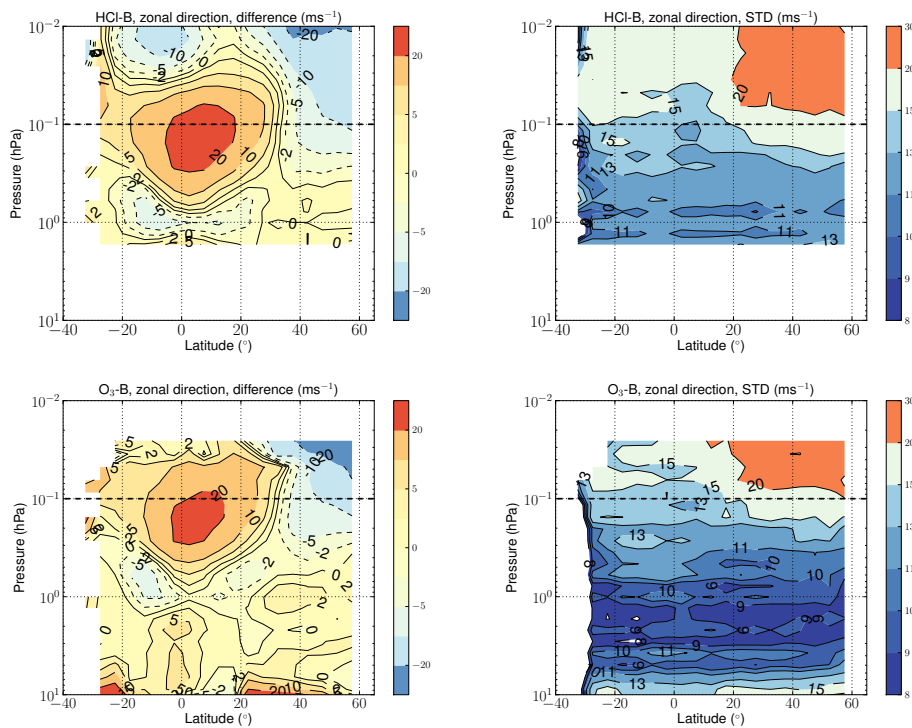


Fig. 8. Same as for Fig. 7 but for the zonal component.

SMILES winds

P. Baron et al.

Title Page

Abstract

Introduction

Conclusions

References

Tables

Figures



Back

Close

Full Screen / Esc

Printer-friendly Version

Interactive Discussion

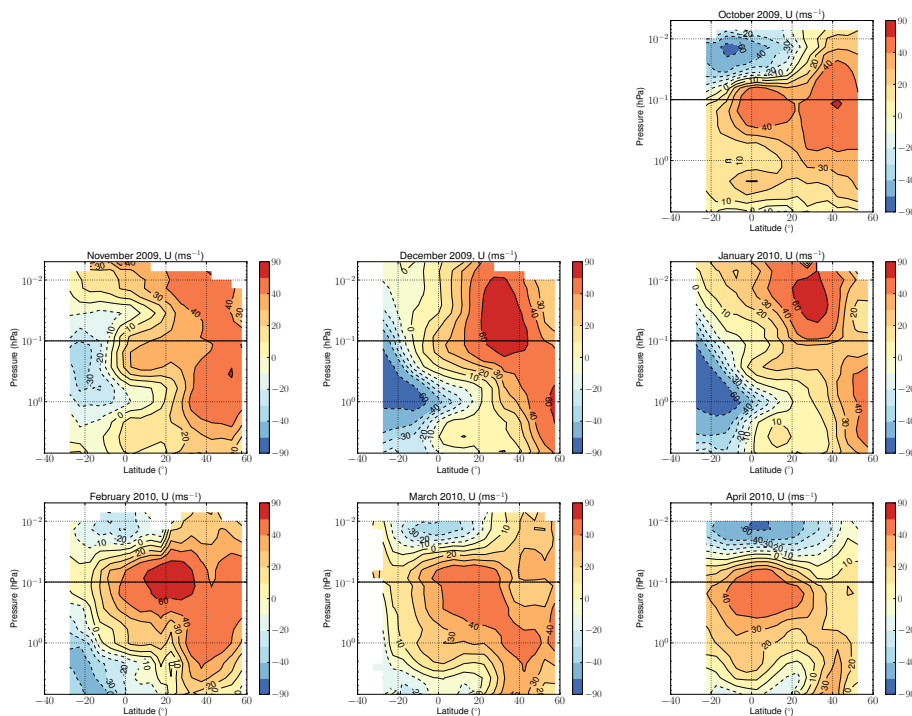


Fig. 9. Monthly and zonally averaged zonal-wind derived from SMILES measurements in band B between October 2009 to April 2010. Wind information is taken from the O_3 line retrieval for altitudes below 0.1 hPa (65 km) and from the HCl line retrieval above.

SMILES winds

P. Baron et al.

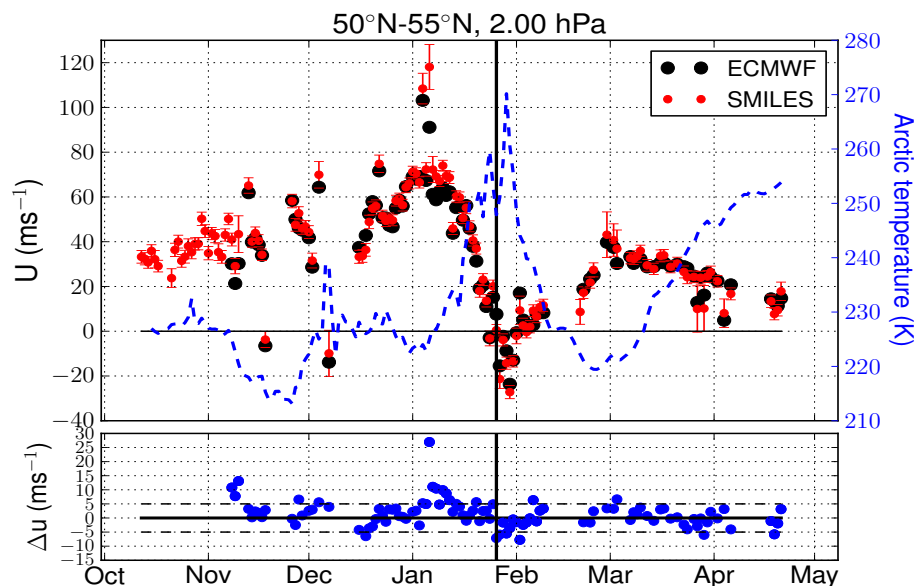


Fig. 10. Upper panel: daily-averaged SMILES zonal-wind in the northern high-latitudes at 2 hPa (~ 41 km) (red dots) and ECMWF analyses (black dots) between 50°N – 55°N . SMILES winds are retrieved from the O_3 line measured in band-B or in band-A if B is not measured. Temperature information (blue dashed line) is based on daily and zonally averaged MLS measurements between 60°N – 80°N . Lower panels: difference SMILES-ECMWF.

[Title Page](#)
[Abstract](#)
[Introduction](#)
[Conclusions](#)
[References](#)
[Tables](#)
[Figures](#)
[◀](#)
[▶](#)
[◀](#)
[▶](#)
[Back](#)
[Close](#)
[Full Screen / Esc](#)
[Printer-friendly Version](#)
[Interactive Discussion](#)

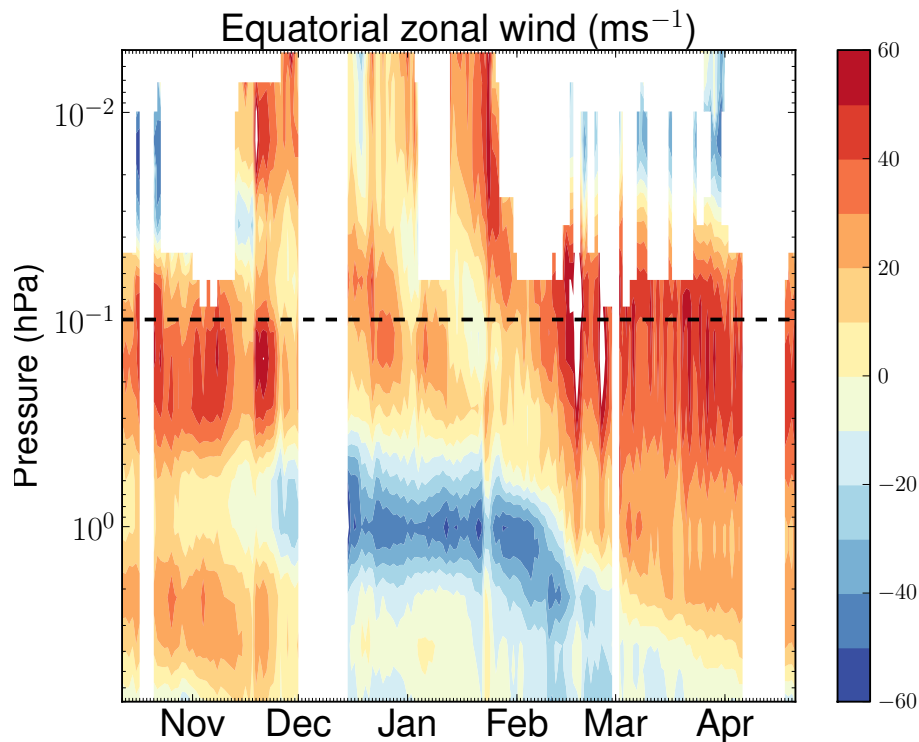



Fig. 11. The Semi-annual oscillation of the zonal winds over the equator ($\pm 5^\circ$). Red regions correspond to eastward (westerly) winds. The winds from both the ozone and HCl lines are combined in the plot when band-B is measured: information is for O_3 line below 0.1 hPa (65 km) and from HCl above. Information is from O_3 when only band-A is measured.

Title Page

Abstract

Introduction

Conclusions

References

Tables

Figures

◀

▶

◀

▶

Back

Close

Full Screen / Esc

Printer-friendly Version

Interactive Discussion



SMILES winds

P. Baron et al.

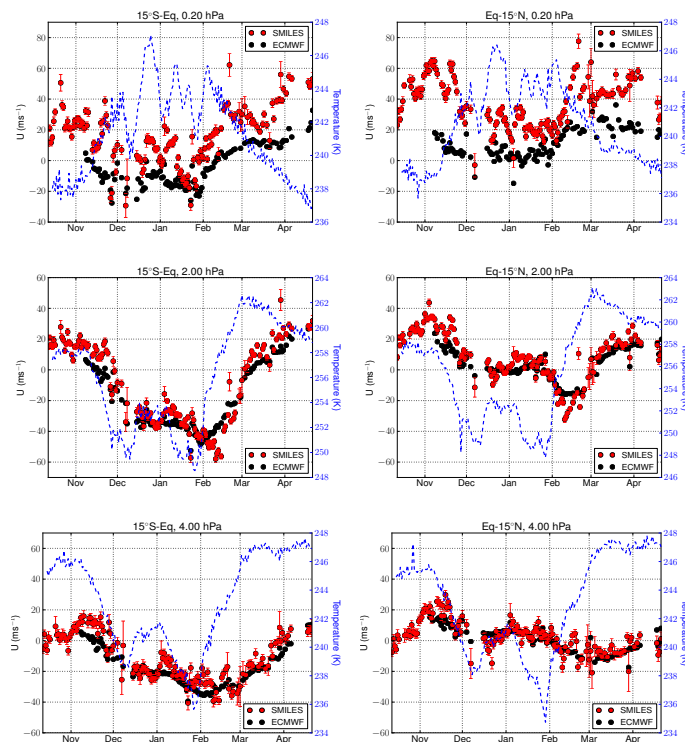


Fig. 12. Left panels: daily-averaged zonal-wind in the southern tropics (15° S–Eq) at 4, 2 and 0.2 hPa (~ 35 , 41 and 60 km) derived from SMILES measurements (red dots) and ECMWF analyses (black dots). Data are retrieved from the O_3 line in band-B or in band-A if B is not measured. The temperature profiles (blue dashed line) is a daily and zonal average of MLS measurements in the same latitudes range. Right panels: same as left panels but for the northern tropics.

[Title Page](#)
[Abstract](#)
[Introduction](#)
[Conclusions](#)
[References](#)
[Tables](#)
[Figures](#)
[◀](#)
[▶](#)
[◀](#)
[▶](#)
[Back](#)
[Close](#)
[Full Screen / Esc](#)
[Printer-friendly Version](#)
[Interactive Discussion](#)
